Effective Field Theory of 2D van Hove Singularities

Anton Kapustin,[1] Tristan McKinney,[1] and Ira Z. Rothstein[2]
[1] *California Institute of Technology, Pasadena, CA 91125*
[2] *Department of Physics, Carnegie Mellon University, Pittsburgh, PA 15213*

We study the effective field theory of 2D fermions with a short-range interaction in the presence of a van Hove singularity. We find that there are additional divergences associated with the singularity that necessitate regularization beyond the usual Wilsonian cut-off. In the full theory these divergences are cut off by the finite size of the Brillouin zone. This leads to a UV/IR mixing and causes the RG equation for the coupling constant to have an explicit dependence on the ratio of the Wilsonian cut-off to the bandwidth. We discuss the properties of the superconducting ground state and the transport properties of the normal state and show that the latter are approximately described by the marginal Fermi liquid scenario. To leading order, our results are universal in the sense that they do not depend upon the nature of the non-van Hove portion of the Fermi surface. We also comment on the van Hove scenario of high-T_c superconductivity.

INTRODUCTION

In the 1990s and early 2000s extensive theoretical work was devoted to the study of systems of 2D fermions with the Fermi level close to a van Hove singularity [1]-[9]. In such a system, the density of states diverges logarithmically thanks to the vanishing of the Fermi velocity at isolated points on the Fermi surface. From the theoretical standpoint, the van Hove singularity is one of the simplest situations in which deviations from the standard Fermi liquid theory are expected. For example, the leading order computation of the self-energy [1, 2] shows that with short-range interaction the width of the quasiparticles is a linear function of energy, a behavior which is characteristic of the Marginal Fermi Liquid (MFL) [10]. Since the MFL paradigm has been proposed to explain some peculiar properties of the normal state of high-T_c superconductors, it was speculated early on that high-T_c superconductors are special due to their proximity to a van Hove singularity [2, 11]. While this scenario fell out of favor, understanding the effect of van Hove singularities on the Fermi liquid remains an important problem.

Most of the studies cited above focus on the 2D Hubbard model on a square lattice at or near half-filling because of its relevance to cuprate superconductors. In this model, the Fermi surface is diamond-shaped and features two inequivalent van Hove points (i.e. points where the Fermi velocity vanishes) as well as nesting. These features complicate the analysis, and it is hard to disentangle the effects of van Hove points and nesting. In this paper we study in detail the case of a single van Hove point from the point of view of Effective Field Theory (EFT). When applied to the case of a non-singular Fermi surface, the EFT approach explains the ubiquity of both the Fermi liquid and BCS-type superconductivity [14]-[15]. The goal of this paper is to extend this systematic approach to systems with a van Hove point at or near the Fermi surface.

We find that the quadratic hyperbolic dispersion law characteristic of electrons near a 2D van Hove point leads to additional divergences not accounted for in the usual Wilsonian approach. The logic of EFT forces us to introduce a Fermi velocity cut-off Υ in addition to the Wilsonian cut-off Λ. Accordingly, the Fermi surface is split into two regions where two different scalings apply: $v_F > \Upsilon$ and $v_F < \Upsilon$. This leads to a renormalizable theory, in the sense that all of the counter-terms are local, but with a peculiar UV/IR mixing: the RG equation for the coupling constant explicitly depends on the ratio of the Wilsonian cut-off Λ to the bandwidth W. This dependence on the UV scale W is only logarithmic, but it has interesting consequences discussed below. The situation is reminiscent of high energy scattering processes, such as the Sudakov form factor, where the phase space of gauge bosons is split into two regions which dominate the IR behavior. This splitting leads to additional (rapidity) divergences which necessitate a new regulator [17] to distinguish between soft and collinear modes. These modes are analogous to the van Hove and non-van Hove regions. Summing contributions from these two sectors leads to a cancellation of the regulator but, as in the present case, the cancellation leaves behind a Cheshire log. This in turn leads to double logs in the renormalization group flow.

Once we have developed the necessary formalism, we utilize it to study how a van Hove singularity modifies the low energy behavior. In particular, we discuss the range of applicability of the MFL scenario and some properties of the superconducting ground state. Since one of the original motivations for the study of such models was high-T_c superconductivity, in the concluding section we briefly discuss whether our findings are in line with the behavior of cuprate superconductors. However, we emphasize that the results of this paper can be applied to a variety of fermionic systems, both naturally occurring (ruthenates) and artificially created (graphene [20]).

While this paper was nearing completion, we became aware of a recent work [21] which addresses the same problem using a similar approach. We comment on the similarities and differences below.

THE ACTION NEAR A VAN HOVE SINGULARITY

The literature on the van Hove (VH) scenario usually takes the 2D Hubbard model on a square lattice near half-filling as the starting point, but the EFT approach is more universal and applies to any system with an "accidental" $O(1,1)$ symmetry at low momenta on some patch of the Fermi surface. We will not assume that the short-range interactions are repulsive as generically they may arise from a combination of Coulomb repulsion and boson-mediated attraction.

Our starting point is an action describing an isolated VH singularity. In the 2D Hubbard model, there are two VH points in the Brillouin zone: $\mathbf{p}_{VH} = (0, \pi)$ and $\mathbf{p}_{VH} = (\pi, 0)$. If the hopping parameters in the x and y directions are unequal, the energies of these two points are different. If the Fermi level is much closer to one of them than the other, it makes sense to study the effective field theory of a single VH singularity. Note that either of the VH points satisfies $2\mathbf{p}_{VH} \sim 0$. This is because each point is fixed by the time-reversal symmetry $\mathbf{p} \mapsto -\mathbf{p}$. In general, if the time-reversal symmetry is present, it can either exchange VH points or leave them invariant. We will assume that time-reversal symmetry is present, and that there is a unique VH point in the Brillouin zone. This forces $\mathbf{p}_{VH}$ to be a fixed point under time-reversal symmetry and thus be equivalent to the origin.

Expanding the nearest-neighbor Hubbard model Hamiltonian around the point $\mathbf{p} = 0$ to lowest order in momentum components and assuming zero-range interaction, the action of the model is

$$S = \int dt\, d^2x \left[\psi^\dagger (i\partial_t - \epsilon(-i\nabla) + \mu)\psi - \frac{g}{2}(\psi^\dagger\psi)^2\right], \quad (1)$$

where the dispersion relation is given by

$$\epsilon(\mathbf{p}) = \mathbf{p}^2 \equiv t_x p_x^2 - t_y p_y^2 \quad (2)$$

and is unbounded from below. Here and below $\mathbf{p}^2$ denotes the square of the 2D vector $\mathbf{p}$ with respect to the indefinite metric $\mathrm{diag}(t_x, -t_y)$. It is convenient to set $t_x = t_y = 1$ by rescaling p_x and p_y; this has the effect of replacing g with $g/\sqrt{t_x t_y}$, while the metric becomes $\mathrm{diag}(1, -1)$. In what follows we redefine g to absorb the factor $1/\sqrt{t_x t_y}$. If we regard p_x, p_y as periodic with period of order 1, then t_x, t_y are of order of the bandwidth W.

As usual, all states with $\epsilon(\mathbf{p}) < \mu$ are assumed to be occupied, so in the free limit $g = 0$ the excitations of the system are particles and holes, both with nonnegative energy. When the Fermi level μ vanishes, the system has a discrete symmetry $\psi \leftrightarrow \psi^\dagger, x \leftrightarrow y$ which exchanges particles and holes.

Let us discuss the symmetries of the model. The quadratic dispersion relation has $O(1,1)$ invariance, and the short-range interaction preserves this symmetry. $O(1,1)$ symmetry can be broken by higher-dimensional operators. The action (1) is also invariant under Galilean boosts, and, for $\mu = 0$, under dilatations

$$\psi(t, \mathbf{x}) \to \lambda^{-1}\psi(\lambda^2 t, \lambda x). \quad (3)$$

Translations, $O(1,1)$ transformations, Galilean boosts and dilatations form the full Schrödinger group [18]. Invariance with respect to Galilean boosts is spontaneously broken by the Fermi sea for all values of μ. Dilation symmetry is anomalous on the quantum level, as we will see below. The internal symmetries of the model include $U(1)$ particle-number symmetry and $SU(2)$ spin symmetry.

THE FULL THEORY

As we shall see below, the model with a quadratic (hyperbolic) dispersion relation is not renormalizable in the sense that at one loop non-local counter-terms are necessitated. Given that the microscopic theory is local, and that the RG flow is local, a sensible EFT must include both the VH region, described by the above model, and the non-VH region, where the Fermi velocity is nowhere vanishing. We use the term "Full Theory" to denote the EFT which includes both regions. We will not make any assumptions about the shape of the Fermi surface in the non-VH region. We will however assume that it is sufficiently featureless that we can define the notion of an average Fermi velocity V_F. As we will show below, our results are universal to leading log accuracy in the sense that they only depend upon V_F and not the detailed shape of the Fermi surface. Therefore our results will apply to any system with a VH singularity with hyperbolic dispersion which is weakly coupled at energies of order the bandwidth.

Since the power counting in the VH and non-VH regions differ, the Fermi surface must be divided into regions, so that each region manifests homogeneous power counting. To define the non-VH region, it is convenient to define $p_\pm = p_x \pm p_y$, so that $\epsilon(\mathbf{p}) = p_+ p_-$. The van Hove region(s) are isolated via a momentum cut-off $|p_\pm| < \Upsilon$, where Υ is much smaller than the size of the Brillouin zone. We also impose the Wilsonian cut-off $|\epsilon(\mathbf{p}) - \mu| < \Lambda$, as usual. The rest of the Fermi surface is the VH region. The choice of Υ and Λ should not affect the physical quantities. We will refer to Υ as the Fermi velocity cut-off. We will see that formally taking the limit $\Upsilon \to \infty$ in the VH region leads to divergences. We will refer to them as "rapidity" divergence because of the aforementioned analogy with high energy scattering theory. Rapidity divergences should be distinguished from UV divergences which arise when one formally takes the limit $\Lambda \to \infty$.

The electron field is decomposed into a van Hove (VH) and a non-VH (N) piece, $\psi = \psi_{VH} + \psi_N$. Then the interaction part of the action can be written as

$$S_{int} = \int \prod_i d^2 p_i dt \left(g_1(p_{i\|}) \psi_N^\dagger(p_1) \psi_N^\dagger(p_2) \psi_N(p_3) \psi_N(p_4) \right.$$
$$+ g_2(p_{1\|}, p_{2\|}) \psi_N^\dagger(p_1) \psi_N^\dagger(p_2) \psi_{VH}(p_3) \psi_{VH}(p_4)$$
$$\left. + \; g_3 \psi_{VH}^\dagger(p_1) \psi_{VH}^\dagger(p_2) \psi_{VH}(p_3) \psi_{VH}(p_4) + h.c. \right) \qquad (4)$$

The momentum-conserving delta-functions have been suppressed. As per the usual power counting, the interactions of the N fields are restricted to the BCS channel, i.e. the momenta are back-to-back, with other interactions being suppressed by powers of E/W. Power counting tells us that g_3 may be regarded as momentum-independent, as in this region all the momenta directions scale to zero as the cut-off is lowered. Furthermore, the couplings g_2 and g_1 match onto g_3 as the momentum approaches the van Hove patch. To leading power g_2 and g_3 can only depend on the components of momenta tangent to the Fermi surface ($p_\|$), since these momenta do not scale as the cut-off is reduced. Also note that the VH-N interaction conserves momentum when the N-particles momenta are restricted to the BCS configuration, since the total momentum of two VH particles is approximately $2\mathbf{p}_{VH} \simeq 0$. In a situation with two VH points exchanged by time-reversal symmetry, momentum conservation would force one of the two VH particles to be associated with one VH point and the other one with the other VH point. That is, for two VH points momentum conservation restricts the "flavor" structure of the interaction.

When the Wilsonian cut-off drops below μ, the linear terms in the dispersion relation $v_F p_\perp$ dominates the quadratic term even in the VH region. Therefore we can integrate out fields with momenta near the VH point, and combine VH and N regions into a single region where only $p_\perp$ is rescaled under RG. Then the Fermi liquid theory applies everywhere on the Fermi surface, with corrections of order Λ/μ.

IS THE THEORY FINELY TUNED?

The basic relations of MFL theory follow directly from the dilatation symmetry and dimensional analysis. However, the dilatation symmetry is both anomalous (i.e. broken by renormalization) and explicitly broken by nonzero μ and higher-dimensional operators. Since the chemical potential is a relevant operator and MFL behavior is predicated on the existence of a nearly vanishing Fermi velocity, we cannot expect MFL behavior to be realized without fine-tuning unless some symmetry protects μ from a large renormalization. Such a symmetry does indeed exist, as the action is invariant under particle-hole interchange for $\mu = 0$. If nonzero μ is the only source of particle-hole symmetry breaking, then the renormalized value of μ differs from the bare value by an amount proportional to μ itself. In other words, a value of μ much smaller than the UV cut-off is technically natural.

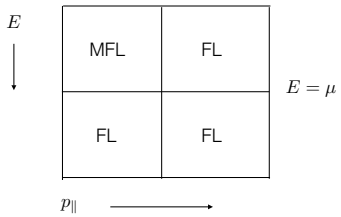

FIG. 1. The behavior of the electron self energy as function of the position on the Fermi surface (horizontal-axis) and energy E. Fermi liquid behavior is regained when the energy drops below the chemical potential. Away from the singularities, FL behavior presides for all energies.

Note that accidental $O(1,1)$ symmetry is present independent of the value of t_x/t_y. When $\mu = 0$ this ratio is RG invariant. For non-vanishing μ this is no longer true, but the effects of renormalization on t_x/t_y will suppressed by powers of μ/W.

The dilatation symmetry is strongly broken at scales of order μ. Thus the model will behave as an MFL at high energies, up to corrections suppressed by powers of μ/E and logarithmic corrections arising from the running of g. In Fig. 1 we show the region in the $E - p_\|$ plane where the MFL behavior applies. Here $p_\|$ denotes a coordinate along the Fermi surface, with a VH point near $p_\| = 0$.

ONE-LOOP RENORMALIZATION

The goal of the Wilsonian EFT approach is to find a formulation of the IR physics which does not depend on the details of the UV physics. To this end one introduces a sliding UV cut-off Λ, integrating out the excitations whose energy is larger than Λ, and retaining only the terms in the action which are not suppressed by powers of Λ. The resulting description is Λ-dependent, but the physical results are Λ-independent once one renormalizes the theory. Higher dimensional operators are then suppressed by the physical scale W. Perturbation theory applies if the coupling $g(\Lambda)$ is small. The potentially dangerous terms enhanced by powers of $\log(\Lambda/E)$, where E is the typical energy scale of the process, can be summed up using RG equations.

Let us consider the running of the coupling beginning in the UV where $\Lambda \gg \mu$. In the non-VH region, we will simplify the problem by taking all the couplings to be

independent of $p_\parallel$. This will be sufficient for our purposes, because we are interested in the behavior of quasiparticles near the VH point. The non-VH region is of interest to us only because the separation of the Fermi surface into VH and non-VH region is somewhat arbitrary, and to account for this we need to study the dependence of our results on the Fermi velocity cut-off Υ.

In the non-VH region one expands the energy $\epsilon(\nabla)$ to linear order in $p_\perp$, the component of momentum normal to the Fermi surface. The Fermi velocity depends on the parameter $p_\parallel$ along the Fermi surface. The interactions are technically irrelevant for almost all kinematic situations. The only two exceptions are the forward channel and the BCS channel [12–14]. The BCS channel (two incoming particles with momenta $\mathbf{p}$ and $-\mathbf{p}$) is particularly important because it can lead to the superconducting instability. The beta-function equation for the BCS coupling has the form [12–15]:

$$\Lambda \frac{dg}{d\Lambda} = N_F g^2, \tag{5}$$

where N_F is the density of states at the Fermi level:

$$N_F = \int \frac{d^2p}{(2\pi)^2}\, \delta(\epsilon(\mathbf{p})) = \frac{1}{4\pi^2} \int dp_\parallel \frac{1}{|v_F(p_\parallel)|}. \tag{6}$$

In the non-VH region the Fermi velocity is nonzero and scales linearly with $p_\parallel$. However, since v_F vanishes at the VH point, the density of states over the entire Fermi surface diverges. We introduce a Fermi velocity cutoff Υ which prevents the loop integrals from sampling the states in the region where the Fermi velocity is below Υ (the VH region).

Then the density of states in the non-VH region is given, with logarithmic accuracy, by

$$N_F(\Upsilon) \simeq \frac{1}{4\pi^2} \log \frac{V_F^2}{\Upsilon^2}. \tag{7}$$

where V_F is the typical Fermi velocity in the non-VH region. The Υ-dependence of both the density of states and the beta-function is not physically acceptable, since the leading-order beta-function is a physical quantity, while Υ is arbitrary. The remnant Υ dependence is a consequence of the fact that we have not fully reproduced the IR physics of the theory. To eliminate the Υ dependence we must include the contribution from the VH region.

Evaluating the particle-particle scattering amplitude at one loop, in the VH region we find with logarithmic accuracy:

$$\mathcal{A}_{VH}(E) = \frac{g^2}{8\pi^2} \left[-2 \log \frac{2\Lambda}{E} \log \frac{2\Lambda}{\Upsilon^2} + \log^2 \frac{E}{2\Lambda} + i\pi \log \frac{\Upsilon^2}{E} \right], \tag{8}$$

where we have kept only the leading terms in the real and imaginary parts.

The amplitude gets contributions both from the two diagrams shown in figure (2). We refer to the two diagrams as the "s-channel" (particle-particle) and the "t-channel" (particle-hole) contributions respectively. The Fermi velocity cut-off Υ dependence comes entirely from the s-channel. Equation (8) has two unusual features: the imaginary part of the amplitude is Υ-dependent, and the logarithmic derivative of the real part with respect to Λ is also Υ-dependent (and divergent if one tries to take the limit $\Upsilon \to \infty$).

Now let us add the contribution of the non-VH region, also evaluated with logarithmic accuracy:

$$\mathcal{A}_N(E) = \frac{g^2}{8\pi^2} \left[-2 \log \frac{2\Lambda}{E} \log \frac{\Upsilon^2}{V_F^2} + i\pi \log \frac{V_F^2}{\Upsilon^2} \right]. \tag{9}$$

This expression is valid provided $E \ll \Lambda$ and we have kept only the Υ dependent pieces.

In the sum, the Υ-dependent terms cancel, as they should, but the amplitude still depends on Λ. Adding the tree-level contribution $-g$ and requiring the total amplitude to be independent of Λ, we find the following RG equation (with logarithmic accuracy):

$$\Lambda \frac{dg}{d\Lambda} = \frac{g^2}{4\pi^2} \log \frac{V_F^2}{\Lambda}. \tag{10}$$

An unusual feature of this equation is that the beta-function has an explicit dependence on Λ, as well as V_F^2. The latter can be regarded as an energy scale of order of the bandwidth, $V_F^2 \sim W$. Thus the IR physics retains some information about the UV scale W. This is a form of UV/IR mixing.

In the special case $\Upsilon^2 = \Lambda$ our scheme in the VH region resembles that of [5]. In that work it is implicitly assumed that g is repulsive, and that Λ can be taken as high as the bandwidth, so that the non-VH region is effectively absorbed into the VH region. If one wants g to account for both Coulomb repulsion and electron-phonon interaction, one needs to keep Λ below the Debye energy, and then it is essential to use two different EFTs in the VH and non-VH regions.

HIGHER ORDER RENORMALIZATION

Let us discuss how higher-order corrections modify these results. Specifically, one may wonder whether the all-order beta-function contains higher powers of $\log(V_F^2/\Lambda)$. (We will call logs containing V_F^2, such as $\log(V_F^2/E)$ or $\log(V_F^2/\Lambda)$, the rapidity logs.) To answer this question, we can use the optical theorem which reads [16]:

$$2\,\mathrm{Im}\mathcal{A}(a \to a) = \sum_X |\mathcal{A}(a \to X)|^2.$$

Any state X on the right-hand side is referred to as an intermediate state. One can then reconstruct the whole

FIG. 2. The diagram on the left/right is referred to as the s/t channel diagram. Not shown is the u channel; diagram which is given by the t channel diagram with the final state particle interchanged.

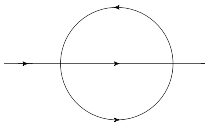

FIG. 3. The two-loop self energy with finite imaginary part.

amplitude using a dispersion relation, up to a counterterm. Summation over intermediate states results in factors of the density of states, at a specified net momentum and energy.

Let us use the optical theorem to re-derive the one-loop beta-function. We choose the initial state a to be the two-particle state with energy E and zero net momentum. The unitarity cut of the one-loop s-channel scattering diagram gives the two-particle intermediate state, while the cuts of the t and u-channel diagrams (see Fig. 2) give particle-hole states. It is easy to see that the two-particle phase space at zero total momentum is logarithmically divergent within our model. Imposing the Fermi velocity cut-off at $V_F \sim \sqrt{W}$, the two-body phase space is simply the one-particle density of states and is of order $\log(V_F^2/E)$, where E is the total energy. The particle-hole phase space vanishes, since a particle-hole system cannot have zero net momentum. Thus the imaginary part of $\mathcal{A}(E)$ at one loop is of order $g^2 \log(V_F^2/E)$. Using the dispersion relation, it is easy to show that the amplitude itself contains logs of the form $g^2(\log(V_F^2/E)\log(\Lambda/E) - \frac{1}{2}\log^2(\Lambda/E))$. Hence the one-loop beta-function contains a rapidity log $g^2 \log(V_F^2/\Lambda)$. This method of derivation makes the connection between the van Hove singularity in the density of states and the log-enhanced terms in the beta-function particularly transparent.

Let us now analyze two-loop contributions to the beta-function. We will be concentrating on the VH region by taking $\Upsilon \sim V_F^2$ in which case there will be no large rapidity logs in non-VH loops. The renormalized coupling g is related to the bare coupling g_b by

$$g_b = g Z_4 Z_2^{-2}, \tag{11}$$

where Z_4 is the renormalization factor for the particle-particle 4-point amplitude, and Z_2 is the wave-function renormalization. Z_2 is finite at one loop, and at two-loop order is determined from the on-shell behavior of the self-energy diagram Fig. 3 whose imaginary part is finite for $\mathbf{p}^2 \neq 0$ [1, 2] and therefore does not contain rapidity logs. As for Z_4, at two-loop order it is computed

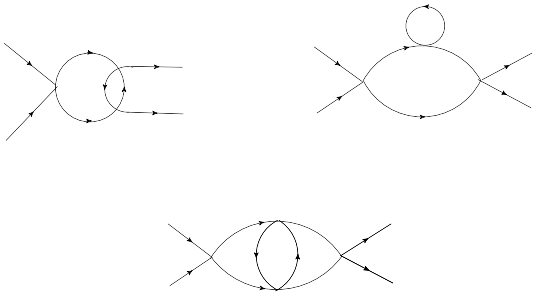

FIG. 4. The top row shows the two loop contributions to the beta function. The diagram with iterated loops is not shown. The second row shows the diagram responsible for the large double rapidity log in the beta function. There exist other three-loop diagrams, but they will not contain double rapidity logs.

from the top two diagrams in Fig. 4 and the iteration of the one-loop s-channel diagram in Fig. 2. The divergences in the latter diagram are absorbed into the one-loop renormalization of g, so the two-loop contribution to the beta-function can come only from the diagrams in Fig. 4 . These diagrams have unitarity cuts with a two-particle intermediate state at zero momentum, and thus their imaginary parts may contain a single rapidity log of the form $g^3 \log(V_F^2/E)$. The corresponding contribution to the beta-function is of the form $g^3 \log(V_F^2/\Lambda)$. We conclude that with logarithmic accuracy the two-loop beta-function has the form

$$\beta(g) = \frac{1}{4\pi^2}(g^2 + Cg^3)\log\frac{V_F^2}{\Lambda}, \tag{12}$$

where C is a constant.

Double rapidity logs in the beta-function could appear for the first time at three loops. Indeed, the bottom diagram in Fig. 4 has two distinct unitarity cuts with zero-momentum two-particle intermediate state, and thus its imaginary part could contain a double rapidity log $g^4 \log^2(V_F^2/E)$. It would lead to a contribution to the beta-function of the form $g^4 \log^2(V_F^2/\Lambda)$.

Notice that our power counting is such that $g\log^2(V_F^2/\Lambda) \sim 1$ but $g\log(V_F^2/\Lambda) \ll 1$, thus the corrections to the beta function coming from the three-loop diagram are suppressed. Thus while in principle these double logs are very interesting, for our purposes they are not important.

Let us compare our results with those of Ref. [21]. These authors also noted that a Fermi velocity cut-off Υ (denoted by K in [21]) is needed to get a finite result for the s-channel diagram shown in figure (2). With the Fermi velocity cut-off in place, the contribution to the beta-function for from this diagram is proportional to $\log(\Upsilon^2/\Lambda)$. This agrees with our results. However, we stress that this Υ-dependence in the beta-function and other quantities is unphysical. In any real model, there must also be a non-VH region, where the dispersion law

deviates from the quadratic form, and there is a cancellation of Υ-dependence between VH and non-VH regions. Further, by choosing Υ to be the typical Fermi velocity in the non-VH region, we can make the contribution of the VH region to various quantities logarithmically enhanced compared to the non-VH region. These logarithmically enhanced terms are model-independent and can be summed using the renormalization group. The one-loop computation suffices to sum up the leading double logs of the form $g^2 \log(\Lambda/E)\log(V_F^2/\Lambda)$. As explained above, at higher orders double rapidity logs in the beta-function and triple logs in the observables might occur, but they are parametrically small in the region where the leading double logs are still under control.

Including the non-VH region is important for the t-channel diagram as well. The authors of [21] found that the logarithmic derivative of this diagram with respect Λ is non-analytic in spatial momentum at zero transfer momentum and $\mu = 0$. The authors interpret this as an inherent non-locality of the theory at $\mu = 0$. However, this non-analyticity depends upon the rapidity cut-off Υ and therefore is unphysical. To demonstrate this, in the appendix we calculate the t-channel diagram using a hard cut-off on momentum (which is distinct from the choice made in [21]) and find a different result for the Υ-dependent non-analyticity. Given that the physical model, which includes the non-VH region, gives Υ-independent results, these non-analyticities will cancel with the non-VH contribution for any physical observable by construction. The $\Upsilon \to \infty$ limit of the t-channel diagram is finite even if we set $\mu = 0$, and therefore the model including both VH and non-VH regions is renormalizable.

SUPERCONDUCTING INSTABILITY

Let us now consider the RG evolution of the coupling from the UV scale Λ_0 down to some IR scale Λ. We assume that Λ_0 is still larger than μ. The solution to the RG equation is

$$g(\Lambda) = \frac{g(\Lambda_0)}{1 + \frac{g(\Lambda_0)}{8\pi^2}\left(\log^2 \frac{\Lambda}{V_F^2} - \log^2 \frac{\Lambda_0}{V_F^2}\right)}. \qquad (13)$$

We see that if the interaction is attractive at the scale Λ_0, i.e. $g_0 = g(\Lambda_0) < 0$, then strong coupling is reached at the scale

$$\Lambda_*^{>} = V_F^2 \exp\left(-\sqrt{\log^2 \frac{V_F}{\Lambda_0} + \frac{8\pi^2}{|g_0|}}\right). \qquad (14)$$

If the strong coupling scale $\Lambda_*^{>}$ is below μ then at $\Lambda = \mu$ we need to match to the usual Fermi liquid EFT and continue running. Solving eq. (5)

$$g(\Lambda) = \frac{g(\mu)}{1 + \frac{g(\mu)}{4\pi^2}\log\frac{\mu}{\Lambda}} \qquad (15)$$

and using the solution (13) for $\Lambda = \mu$ as a boundary conditions gives

$$\Lambda_*^{<} = V_F^2 \exp\left(-\frac{4\pi^2}{|g_0|} - \log\frac{V_F^2}{\mu} + \frac{1}{2}\log^2\frac{V_F^2}{\mu} - \frac{1}{2}\log^2\frac{V_F^2}{\Lambda_0}\right), \qquad (16)$$

where we have assumed again that $g_0 < 0$.

As in the ordinary BCS theory [27] the strong coupling scale is non-perturbative in g_0, however the dependence of the strong-coupling scale on the microscopic parameters differs from (16). Note that (16) simplifies if we set $\Lambda_0 = V_F^2 \sim W$. But this choice may be unphysical if the van Hove EFT is obtained by integrating out some other degrees of freedom at a scale below W. For example, if the short-range interaction arises both from the screened Coulomb repulsion and the phonon-mediated attraction, the van Hove EFT applies only up to energy scales of order the Debye frequency ω_D, which is usually much smaller than the bandwidth W. Then the natural choice for Λ_0 is ω_D, and we have a hierarchy of scales $V_F^2 \simeq W \gg \omega_D$.

Let us now calculate the zero-temperature gap. When calculating the effective potential [15] we couple two distinct gap functions Δ_{VH} and Δ_N to the two bilinears $\psi_{VH}\psi_{VH}$ and $\psi_N\psi_N$, respectively. In general these functions depend upon $p_\parallel$ as well as the rapidity cut-off Υ. The effective potential $V[\Delta_{VH}(p_\parallel, \Upsilon), \Delta_N(p_\parallel, \Upsilon)]$ is by construction independent of Υ. Furthermore we have the boundary condition $\Delta_{VH}(\Upsilon, \Upsilon) = \Delta_N(\Upsilon, \Upsilon)$. By choosing $\Upsilon \sim V_F$, there will be no contribution to the effective potential from the non-VH sector to leading log accuracy. The non-VH sector will develop a gap as well but its scale will not be enhanced as in is the case in for the VH gap. This hierarchy between gaps deserves further exploration.

In our approximation $|\Delta| \equiv |\Delta_{VH}|$ is constant, because it couples to the fields living near a single van Hove point, and we are Taylor-expanding all quantities to leading order around this point. In particular, one should not interpret the fact that $|\Delta|$ is momentum-independent as a sign that the gap is an S-wave, since elsewhere on the Fermi surface the gap function might vanish.

The gap equation has both the UV divergence arising from integration over $|\epsilon(\mathbf{p})|$ and the rapidity divergence. We regulate the UV divergence by restricting the integration range to $|\epsilon(\mathbf{p})| < \Lambda$. The rapidity divergence is regulated using the Fermi velocity cut-off $\Upsilon \simeq V_F$. If g is small, we can solve the gap equation as follows. The gap equation is given by [27]

$$\frac{1}{g} = -\frac{1}{2}\int \frac{d^2p}{(2\pi)^2}\frac{1}{\sqrt{\epsilon(\mathbf{p})^2 + |\Delta|^2}} = -\frac{1}{2}\int_{-\Lambda}^{\Lambda} dE \frac{N_F(E)}{\sqrt{E^2 + |\Delta|^2}}, \qquad (17)$$

where $N_F(E)$ is the density of states near $E = 0$:

$$N_F(E) \;=\; \int \frac{d^2p}{(2\pi)^2}\delta(E - \mathbf{p}^2) \;=\; \frac{1}{4\pi^2}\log\frac{V_F^2}{|E|}. \quad (18)$$

One can evaluate the integral on the r.h.s. of (17) with logarithmic accuracy assuming that $|\Delta| \ll \Lambda \ll V_F^2$. Solving for Δ, we find

$$|\Delta| \simeq 2V_F^2 \exp\left(-\sqrt{\log^2\frac{V_F^2}{\Lambda} + \frac{8\pi^2}{|g|}}\right) = 2\Lambda_*^>.$$

If $g(\Lambda)$ is small, this is nonperturbatively small, so the assumption $|\Delta| \ll \Lambda \ll V_F^2$ is justified.

We can estimate the superconducting transition temperature T_c similarly by solving the temperature-dependent gap equation and using the fact that at $T = T_c$ the gap vanishes. If we assume that $\mu \ll T_c$, the equation for T_c becomes

$$\frac{1}{g} = -\frac{1}{2}\int \frac{d^2p}{(2\pi)^2}\frac{\tanh\frac{|\epsilon(\mathbf{p})|}{2T_c}}{|\epsilon(\mathbf{p})|} = \\ -\frac{1}{2}\int_{-\Lambda}^{\Lambda}\frac{dE}{|E|}N_F(E)\tanh\frac{|E|}{2T_c}. \quad (19)$$

Assuming that $T_c \ll \Lambda \ll V_F^2$ and evaluating the integral with logarithmic accuracy, we find

$$T_c \simeq \frac{2e^\gamma}{\pi}\,\Lambda_*^>, \quad (20)$$

where $\gamma = 0.577...$ is the Euler's constant. In particular, we get the same relation as in the BCS theory:

$$|\Delta| \simeq \frac{\pi}{e^\gamma}T_c \simeq 1.76\;T_c. \quad (21)$$

The above results also apply if μ is smaller than $\Lambda_*^>$. If $\mu \gg \Lambda_*^>$, then at the scale μ the coupling is still weak and we have to match to the usual EFT for the Fermi liquid [12–15]. Then T_c can be determined in the usual way using μ as the UV cut-off. The coupling at the scale μ is given by (13).

While the universal BCS relation $|\Delta| \simeq 1.76\,T_c$ is preserved in our model, the dependence of Δ and T_c on the microscopic parameters such as g_0 and ω_D is altered compared to the usual theory. In particular, the isotopic effect is reduced. Indeed, while in the usual theory the exponent governing the isotopic effect is

$$\alpha = \frac{1}{2}\omega_D\frac{\partial}{\partial\omega_D}\log T_c = \frac{1}{2},$$

in our model we get (after setting $\Lambda = \omega_D$):

$$\alpha = \frac{1}{2}\omega_D\frac{\partial}{\partial\omega_D}\log T_c = \frac{1}{2}\frac{\log\frac{V_F^2}{\omega_D}}{\log\frac{V_F^2}{0.88T_c}}. \quad (22)$$

Thus the effect of the VH singularity is to lessen the isotopic effect in comparison to the standard BCS theory.

QUASI-PARTICLE WIDTH

One of the defining properties of the MFL is that the quasi-particle width, defined via the imaginary part of the on-shell self-energy, is proportional to energy. In our model it receives contributions both from the VH and non-VH regions. For energies much larger than μ the VH contribution can be determined from scaling symmetry and dimensional analysis and is proportional to E . The leading contribution occurs at two loops and is of order [1, 2]

$$\Gamma(E) \sim g^2 E. \quad (23)$$

Unlike in the particle-particle scattering amplitude, there are no additional divergences from the integration over the Fermi surface, and no log enhancement. The non-VH contribution scales as g^2E^2/W, as usual, and is suppressed relative to the VH contribution when $E \ll W$. If $\mu \neq 0$, numerical evaluation of an explicit formula for the imaginary part of self-energy, eq. (17) of [1], indicates that there are also small corrections to $\Gamma(E)$ of order $g^2\mu\log\frac{|\mu|}{E}$. Thus the quasi-particle width is approximately linear in E in the range $|\mu| \ll E \ll \omega_D$.

Since renormalization breaks scaling symmetry, higher-order perturbative corrections affect this result. At leading log accuracy, the effect of higher-order corrections can be included by replacing g with a running coupling $g(E)$:

$$\Gamma(E) \sim g^2(E)E, \quad (24)$$

where $g(E)$ is given by eq. (13).

THE VAN HOVE SINGULARITY AND THE PHYSICS OF CUPRATES

Let us now make contact with the prior work connecting van Hove singularity with the Marginal Fermi Liquid and normal state properties of the high-T_c superconductors. One important property of cuprate superconductors is that the normal state resistivity grows linearly with temperature. This is often interpreted as a signature of fermionic quasi-particles whose width grows linearly with energy. In contrast, in the normal Fermi liquid the quasi-particle width scales as E^2.

In the van Hove EFT, the MFL behavior is expected for $\mu = 0$. Indeed, the model has scaling symmetry on the classical level which forces the imaginary part of self-energy to scale as E for all energies. On the quantum level, there are deviations from the linear scaling because the coupling constant runs, or equivalently because the theory develops a strongly coupled scale $\Lambda_*^>$. But if the relevant energy scale is well above $\Lambda_*^>$, weak coupling prevails and radiative corrections are small. For $\mu \neq 0$ the approximately linear behavior is expected only for

energies in the range $\mu \ll E \ll \omega_D$, where we assume that $\omega_D \ll V_F^2$.

The MFL behavior is expected only for quasi-particles whose momentum is in the region where the dispersion law has approximate $O(1,1)$ symmetry. For quasi-particles away from the van Hove region, the usual Fermi liquid scaling applies, and the width is much smaller (scales as E^2).

ARPES studies of cuprate superconductors show that the width of quasi-particles depends strongly on the location on the Fermi surface, with quasi-particles being very narrow in the nodal region and wide in the anti-nodal region [22]. This behavior manifests itself in "Fermi-arcs" when the intensity is plotted as a function of momentum and it is broadly consistent with the van Hove scenario. However, the available fits to the ARPES data [23] show that the condition $\mu \ll V_F^2$ is not satisfied , except perhaps for a very narrow range of dopings. This makes the applicability of the van Hove scenario to such materials questionable.

Another important feature observed in many experiments is a large angle-dependent gap known as the pseudogap [24]. The pseudogap is much larger than T_c. This has no counterpart in the van Hove or MFL scenario, which apart from the bandwidth W only has a single low-energy scale, namely T_c.

The isotopic effect in cuprate superconductors has the same sign as in the BCS theory, but is much reduced near optimal doping [25]. This is broadly consistent with eq. (22).

It is firmly established by now that the superconducting gap in high-T_c superconductors has a d-wave symmetry, vanishing in the nodal (π,π) direction and having opposite signs in the $(0,\pi)$ and $(\pi,0)$ directions [26]. Such a behavior cannot be addressed within our model, because we essentially study the neighborhood of a single van Hove point (say, $(\pi,0)$). It might be possible to obtain a gap with the right symmetry in a model with two van Hove points.

Our conclusion is that while the van Hove scenario is broadly consistent with some features of high-T_c superconductors, it is not clear that it can capture all the relevant physics. On the other hand, the van Hove EFT, due to its universality, applies to other systems with a van Hove singularity and a short-range interaction. The formalism might also be generalized to study Fermi systems with other non-canonical dispersion relations.

APPENDIX: THE PARTICLE-HOLE DIAGRAM

In this appendix we show that the particle-hole exchange contribution (second diagram in figure (2)) does not lead to any non-local behavior in the low energy theory. After doing the energy integral by contours and changing coordinates to $k_\pm = k_x \pm k_y$, we get

$$\Gamma_{ph} = -\frac{1}{2} g^2 \int \frac{d^2k}{(2\pi)^2} \frac{f_+ - f_-}{\epsilon(k) - \epsilon(k+q)} \times \theta(\Lambda - |\epsilon(k)|)\theta(\Upsilon - |k_+|)\theta(\Upsilon - |k_-|), \quad (25)$$

where

$$f_+ = \theta(-\epsilon(k) + \mu)\theta(\epsilon(k+q) - \mu)$$

and

$$f_- = \theta(\epsilon(k) - \mu)\theta(-\epsilon(k+q) + \mu).$$

To determine if this expression leads to a non-locality and failure of renormalizability, we differentiate with respect to the cut-off. The derivative only acts on the step-functions constraining the energy:

$$\frac{d\theta(\Lambda - |\epsilon(k)|)}{d\Lambda} = \delta(\Lambda - k_+k_-)\theta(\Lambda + k_+k_-) + \theta(\Lambda - k_+k_-)\delta(\Lambda + k_+k_-).$$

Using the delta functions to perform the k_+ integral yields

$$\frac{d\Gamma_{ph}}{d\Lambda} = -\frac{g^2}{8\pi^2}\left(\frac{1}{q}\right)\int \frac{dk}{|k|}\left[\frac{\theta(-\Lambda + q(-\Lambda/k + k + q) - \mu)}{\Lambda/k - k - q} + \frac{\theta(-\Lambda - q(\Lambda/k + k + q) + \mu)}{\Lambda/k + k + q}\right] \times \theta(\Upsilon - |\Lambda/k|)\theta(\Upsilon - |k|), \quad (26)$$

where the components of the momentum transfer are assumed to be $q_+ = q_- = q > 0$. We rewrite the step-functions involving q as

$$\theta(-\Lambda + q(-\Lambda/k + k + q) - \mu) = \theta(k - \kappa_{A+}) + \theta(-k)\theta(k - \kappa_{A-})$$

and

$$\theta(-\Lambda - q(\Lambda/k + k + q) + \mu) = \theta(-k + \kappa_{B+}) + \theta(-k)\theta(k - \kappa_{B-}),$$

where

$$\kappa_{A\pm} = \frac{1}{2} y \left(1 \pm \sqrt{1 + \frac{4\Lambda}{y^2}}\right),$$

$$\kappa_{B\pm} = -\frac{1}{2} w \left(1 \pm \sqrt{1 + \frac{4\Lambda}{w^2}}\right),$$

$$y = \frac{\Lambda + \mu}{q} - q$$

$$w = \frac{\Lambda - \mu}{q} + q.$$

Note that if we assume $q \ll \sqrt{\Lambda} \ll \Upsilon$,

$$\kappa_{A+} \approx \frac{\Lambda}{q} \gg \frac{\Lambda}{\Upsilon},$$
$$\kappa_{B+} \approx -\frac{\Lambda}{q} \ll -\frac{\Lambda}{\Upsilon},$$
$$\kappa_{A-} \approx \kappa_{B-} \approx -q \gg -\Upsilon.$$

This implies that several of the step-functions constraining the components of the momentum are redundant. Simplifying the step-functions and performing elementary integrals yields:

$$\Lambda \frac{d\Gamma_{ph}}{d\Lambda} = -\frac{g^2}{8\pi^2}\left(\frac{\Lambda}{q}\right)[(I_{A+}+I_{A-})\theta(q-q_A) + (I_{B+}+I_{B-})\theta(q-q_B)], \quad (27)$$

where

$$I_{A+} = \frac{1}{2\sqrt{\Lambda+q^2/4}} \log\left[\frac{(\eta_1-1)(\eta_2+1)}{(\eta_1+1)(\eta_2-1)}\right], \quad (28)$$

$$I_{A-} = \frac{1}{2\sqrt{\Lambda+q^2/4}} \log\left[\frac{(\eta_3+1)(\eta_4-1)}{(\eta_3-1)(\eta_4+1)}\right], \quad (29)$$

$$I_{B+} = \frac{\phi_1-\phi_2}{\sqrt{\Lambda-q^2/4}}, \quad (30)$$

$$I_{B-} = \frac{\phi_3-\phi_4}{\sqrt{\Lambda-q^2/4}}. \quad (31)$$

The auxiliary quantities in (28)-(31) are

$$\eta_1 = \frac{\kappa_{A+}+q/2}{\sqrt{\Lambda+q^2/4}}$$
$$\eta_2 = \frac{\Upsilon+q/2}{\sqrt{\Lambda+q^2/4}}$$
$$\eta_3 = \frac{\kappa_{A-}+q/2}{\sqrt{\Lambda+q^2/4}}$$
$$\eta_4 = \frac{-\Lambda/\Upsilon+q/2}{\sqrt{\Lambda+q^2/4}},$$

and

$$\phi_1 = \arctan\left(\frac{-\Upsilon+q/2}{\sqrt{\Lambda-q^2/4}}\right)$$
$$\phi_2 = \arctan\left(\frac{\kappa_{B+}+q/2}{\sqrt{\Lambda-q^2/4}}\right)$$
$$\phi_3 = \arctan\left(\frac{\kappa_{B-}+q/2}{\sqrt{\Lambda-q^2/4}}\right)$$
$$\phi_4 = \arctan\left(\frac{-\Lambda/\Upsilon+q/2}{\sqrt{\Lambda-q^2/4}}\right).$$

The momentum step-functions jump at

$$q_A = \frac{1}{2}\left(\Upsilon - \frac{\Lambda}{\Upsilon}\right)\left[\sqrt{1+4\frac{\Lambda+\mu}{(\Upsilon-\Lambda/\Upsilon)^2}}-1\right],$$
$$q_B = \frac{1}{2}\left(\Upsilon + \frac{\Lambda}{\Upsilon}\right)\left[1-\sqrt{1-4\frac{\Lambda-\mu}{(\Upsilon+\Lambda/\Upsilon)^2}}\right],$$

which we can expand to find

$$q_A \approx q_B \approx \frac{\Lambda+\mu}{\Upsilon}.$$

The expression (27) is clearly non-analytic at $q=0$ but it does not diverge there in contrast to Ref. [21]. In fact, it is identically zero in a neighborhood of the origin whose size is of order Λ/Υ. This is true even if we set $\mu = 0$. This neighborhood shrinks to a point if we take the limit $\Upsilon \to \infty$ at a fixed Λ. Outside of this neighborhood, the expression is nonzero, but has a finite $\Upsilon \to \infty$ limit. The convergence to this limit is non-uniform in q. Indeed, for large but finite Υ the first correction to the $\Upsilon = \infty$ limit is of order $\frac{\Lambda}{q\Upsilon}$. For any fixed nonzero q, this goes to zero as $\Upsilon \to \infty$, but one can make this contribution of order 1 if one simultaneously scales down q by keeping it of order Λ/Υ.

The residual Υ dependence must cancel against power suppressed contributions from the NVH region. With this in mind, we shall focus on the limit $\Upsilon \to \infty$ (and fixed nonzero q) and set $\mu = 0$. This yields

$$\Lambda \frac{d\Gamma_{ph}}{d\Lambda} = -\frac{g^2}{8\pi^2}\left(\frac{\Lambda}{q}\right)\theta(q) \times \left\{\left(\frac{1}{2\sqrt{\Lambda+q^2/4}}\right)\log\left[\frac{2\Lambda+q(q-\sqrt{\Lambda+q^2})}{2\Lambda+q(q+\sqrt{\Lambda+q^2})}\right] - \left(\frac{1}{2\sqrt{\Lambda-q^2/4}}\right)\left[\frac{\pi}{2}+\arctan\left(\frac{q}{2\sqrt{\Lambda-q^2/4}}\right) + \arctan\left(\frac{\Lambda-\sqrt{\Lambda^2+6\Lambda q^2+q^4}}{2q\sqrt{\Lambda-q^2/4}}\right) - \arctan\left(\frac{\Lambda+\sqrt{\Lambda^2+6\Lambda q^2+q^4}}{2q\sqrt{\Lambda-q^2/4}}\right)\right]\right\}. \quad (32)$$

This expression is an analytic function of q^2 near $q^2 = 0$ and its Taylor expansion is given by:

$$\Lambda \frac{d\Gamma_{ph}}{d\Lambda} = \frac{g^2}{4\pi^2}\left[1+\frac{q^2}{3\Lambda}-\frac{37q^4}{15\Lambda^2}+\mathcal{O}\left(\frac{q^6}{\Lambda^3}\right)\right]. \quad (33)$$

We conclude that there is no non-locality at zero momentum and $\mu = 0$ as claimed in Ref. [21].

ACKNOWLEDGEMENTS

This work supported by the DOE contracts DE-FG02-92ER40701, DOE-ER-40682-143, and DE-AC02-6CH03000. The authors gratefully acknowledge helpful

conversations with Joe Polchinski, Max Metlitskii, Lesik Motrunich, and Ingmar Saberi. AK and TM are grateful to the Simons Center for Geometry and Physics for hospitality during various stages of this work. AK is also grateful to the Aspen Center for Physics, the Kavli Institute for Physics and Mathematics of the Universe, and Institut des Hautes Etudes Scientifiques for hospitality. IZR is grateful to the Cal-Tech theory group for hospitality and to the Moore Foundation for support.

[1] S. Gopalan, O. Gunnarsson and O. K. Andersen, Phys. Rev. B **46**, 11798 (1992).
[2] P. C. Pattnaik, C. L. Kane, D. M. Newns and C. C. Tsuei, Phys. Rev. B **45**, 5714 (1992).
[3] I. Dzialoshinskii, J. Phys. France **6**, 119 (1996).
[4] J. V. Alvarez, J. Gonzalez, F. Guinea, and M. A. H. Vozmediano, J. Phys. Soc. Jpn. **67**, 1868 (1998) .
[5] D. Menashe and B. Laikhtman, Phys. Rev. B **59**, 13592 (1999)
[6] C. Honerkamp, M. Salmhofer, N. Furukawa, and T. M. Rice, Phys. Rev. B **63**, 035109 (2001).
[7] D. Zanchi and H. J. Schulz, Phys. Rev. B**61**, 13609 (2000) [arXiv:cond-mat/9812303]
[8] C. J. Halboth and W. Metzner, Phys. Rev. B **61**, 7364 (2000) [arXiv:cond-math/9908471];
[9] V. Yu. Irkhin, A. A. Katanin, and M. I. Katsnelson, Phys. Rev. B **64** 165107 (2001) .
[10] C. M. Varma, P. B. Littlewood, S. Schmitt-Rink, E. Abrahams and A. E. Ruckenstein, Phys. Rev. Lett. **63**, 1996 (1989).
[11] For a review of the van Hove scenario see R. S. Markiewicz, J. Phys. Chem. Solids **58**, pp. 1179-1310 (1997); J. Bok and J. Bouvier, in *New Topics in Superconductivity Research*, ed. B. P. Martin, Nova Science Publishers (2006).
[12] G. Benfatto, and G. Gallavoti, Phys. Rev. B **42**, 9967 (1990).
[13] R. Shankar, Physica A **177**, 530 (1991), Rev. Mod. Phys. **66**, 129 (1994).
[14] J. Polchinski, in *Boulder 1992, Proceedings, Recent directions in particle theory* 235-274 [arXiv: hep-th/9210046].
[15] S. Weinberg, Nucl. Phys. B **413**, 567 (1994) [cond-mat/9306055].
[16] S. Weinberg, "The quantum theory of fields. Vol. 1: Foundations," Cambridge University Press, 2005.
[17] J. Y. Chiu, A. Jain, D. Neill and I. Z. Rothstein, Phys. Rev. Lett. **108**, 151601 (2012) [arXiv:1104.0881 [hep-ph]]. J. -Y. Chiu, A. Jain, D. Neill and I. Z. Rothstein, JHEP **1205**, 084 (2012) [arXiv:1202.0814 [hep-ph]].
[18] C. R. Hagen, Phys. Rev. D **5**, 377 (1972).
[19] S. Raghu et al., Phys. Rev. B **79**, 214402 (2009).
[20] R. Nandkishore, L. Levitov, and A. Chubukov, Nature Physics **8**, 158 (2012).
[21] S. Ghamari, S-S. Lee, and C. Kallin, Phys. Rev. B **92**, 085112 (2015).
[22] A. Damascelli, Z. Hussain, and Z-X. Shen, Rev. Mod. Phys. **75**, 473 (2003).
[23] M. R. Norman, M. Randeria, H. Ding, and J. C. Campuzano, Phys. Rev. B **52**, 615 (1995).
[24] T. Timusk and B. Statt, Rep. Prog. Phys. **62**, 61 (1999).
[25] J. P. Franck, in *Physical Properties of High Temperature Superconductors IV,* p.189-293, ed. D. M. Ginsberg, Singapore: World Scientific (1994).
[26] C. C. Tsuei and J. R. Kirtley, Rev. Mod. Phys. **72**, 969 (2000).
[27] R. Schrieffer, *Theory of superconductivity,* Perseus Books, revised edition (1999).